Astrophysical distortion of the large-scale Lyman-alpha forest

arXiv 1402.0506, 1407.6367

THE ROYAL SOCIETY

Simeon Bird (CfA), Hiranya Peiris (UCL), Licia Verde (Barcelona)

Andrew Pontzen

UCL

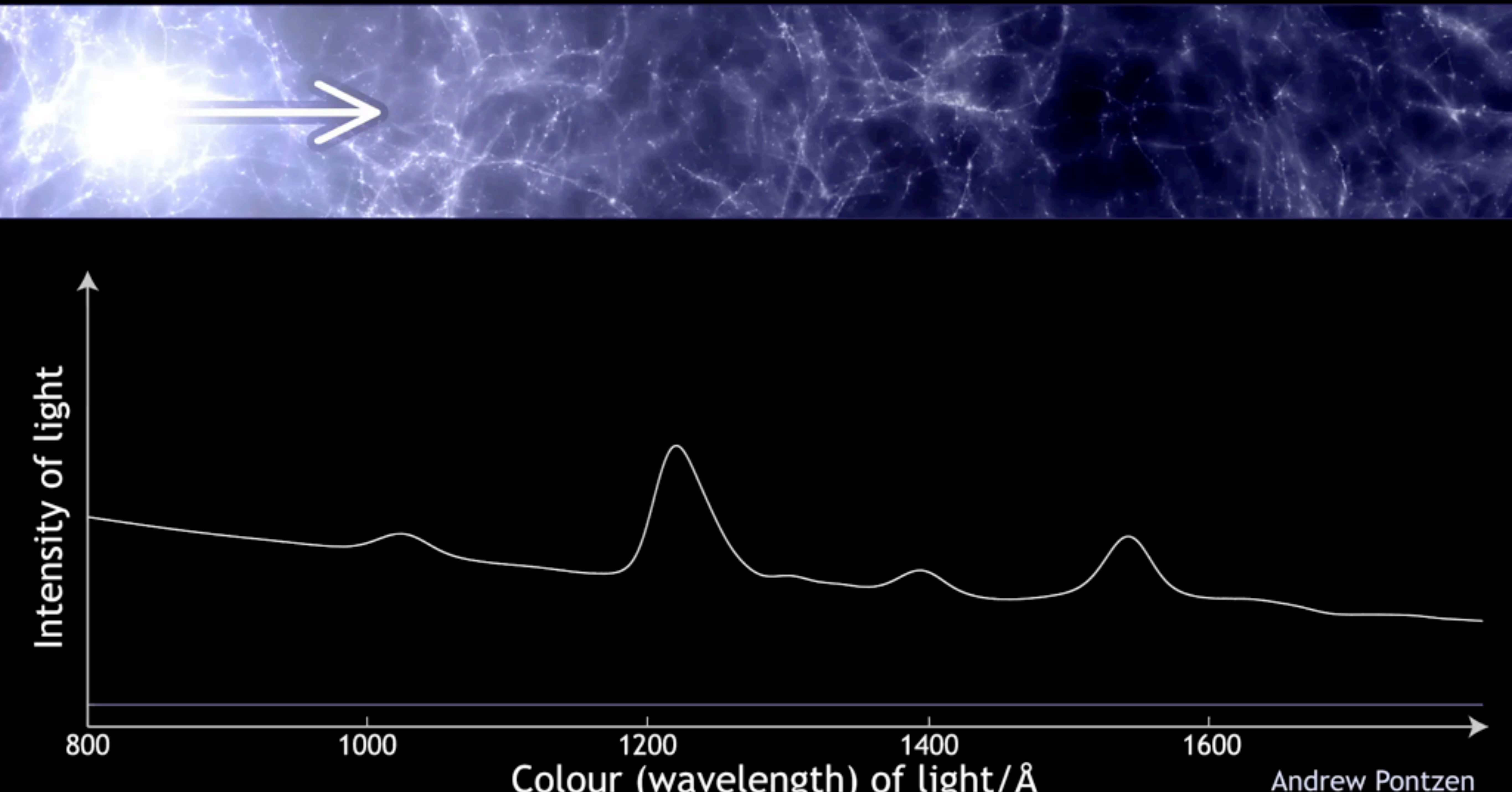
Intensity of light
800
1000
1200
1400
1600
Colour (wavelength) of light/Å
Andrew Pontzen

<z>=2.3 BAO feature

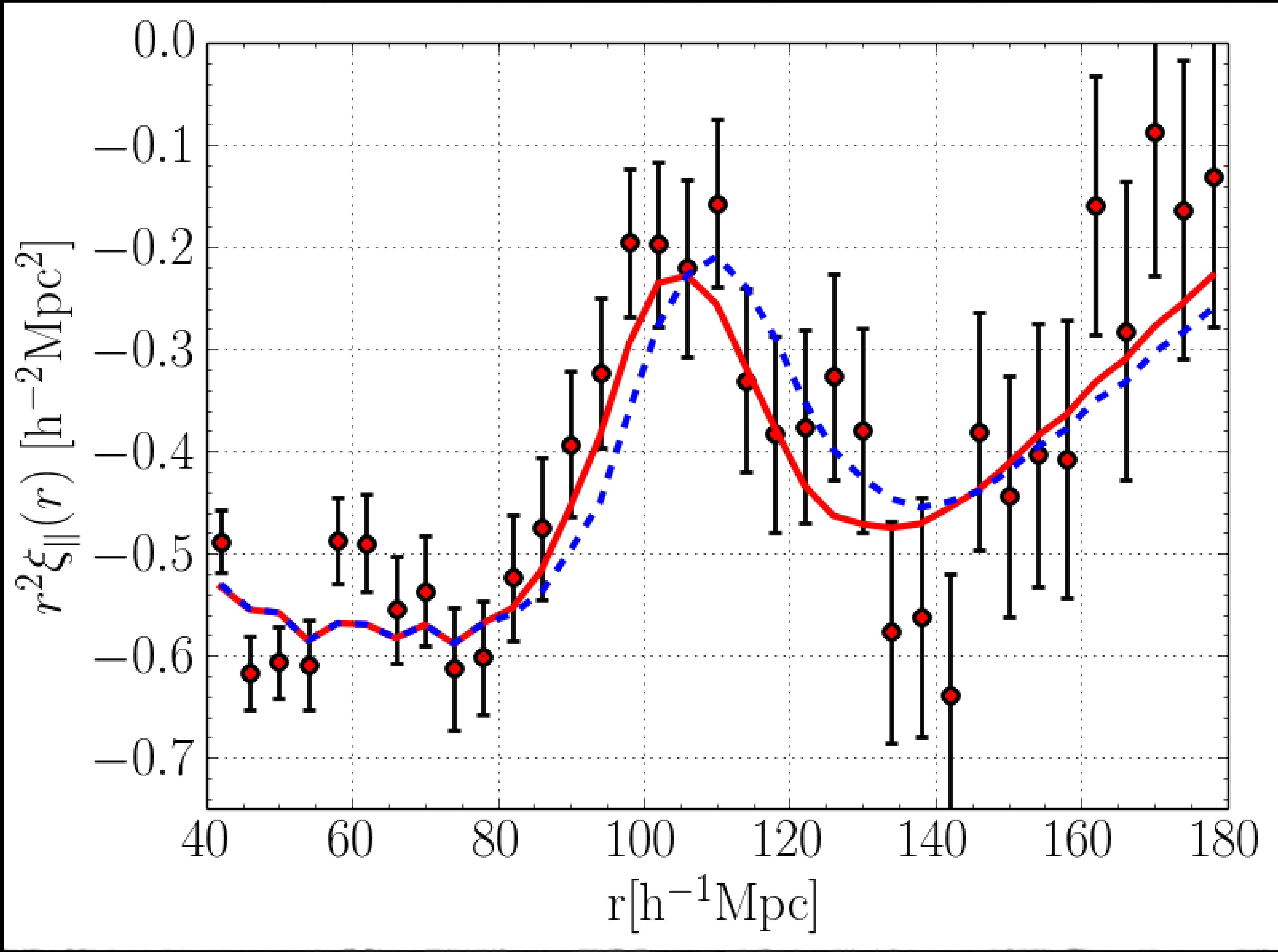

Delubac et al (BOSS collaboration) 2015,
AA; 1404.1801

(12) can actually be

$$^{+3)/2} F_n\left(\frac{r^2}{2(R_1^2 + R_2^2)}\right), \quad (16)$$

s Kummer's function
our previous notation,

$$(17)$$

$$^{+3} F_n\left(\frac{r^2}{4R_s^2}\right), \quad (18)$$

$$\left(\frac{r^2}{2(R_s^2 + R_g^2)}\right). \quad (19)$$

totic behavior, $F_n \to 1$
Thus, for $r \gg R_s$, all
nately equal, demon-
$\approx (1 + \kappa)^2 \xi$ on large
satisfied, our modifi-
l increases the galaxy
les by the same factor.
correlations and the
ly occurs at $r \sim R_s$. Its
nd on the shape of the
nce dependence of a
ssumed Gaussian).
fluctuation spectrum
n both cases, we chose
r values of κ indicated
on of the domain of
upt transition between

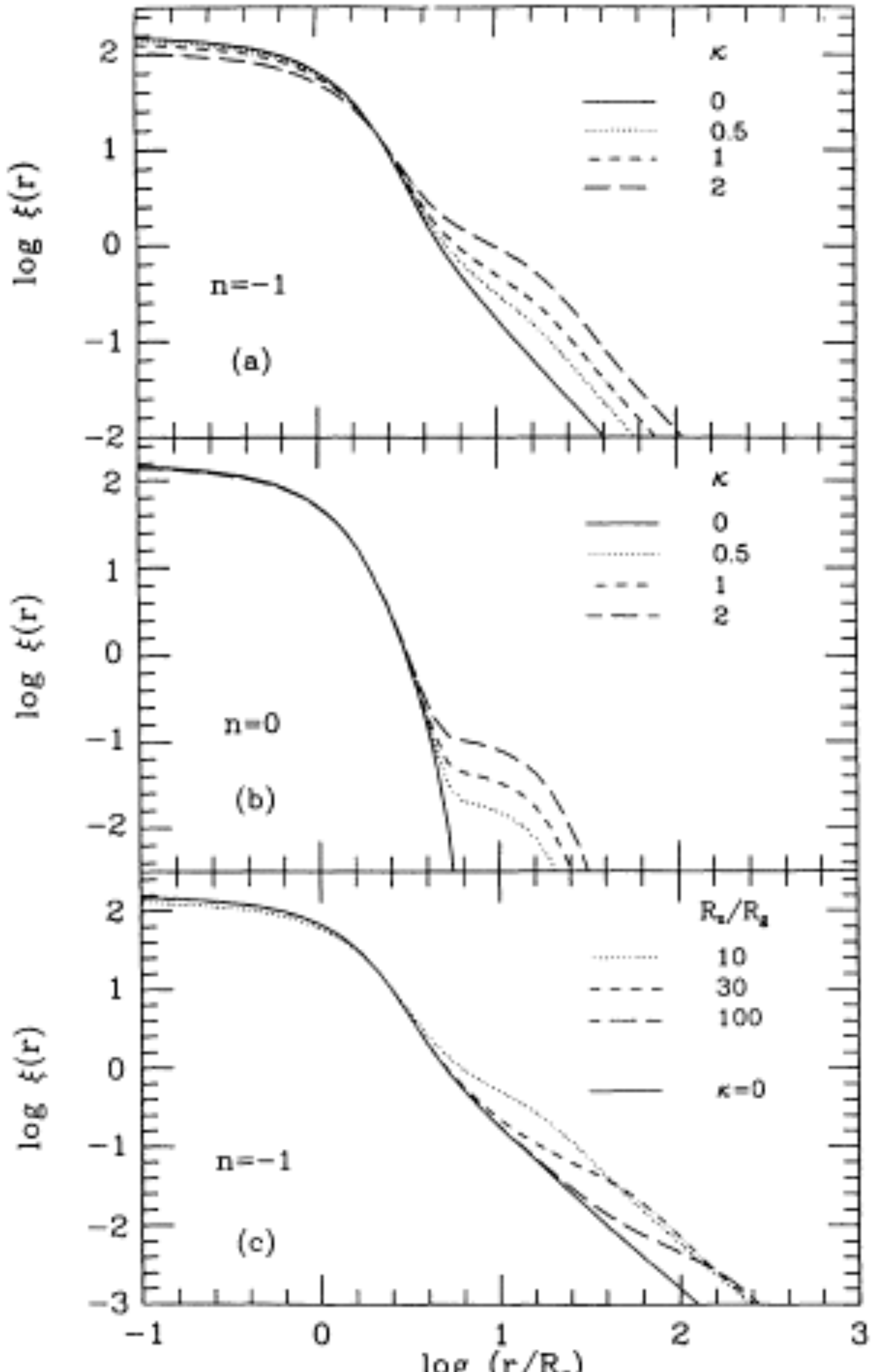

Bower et al
1993, ApJ

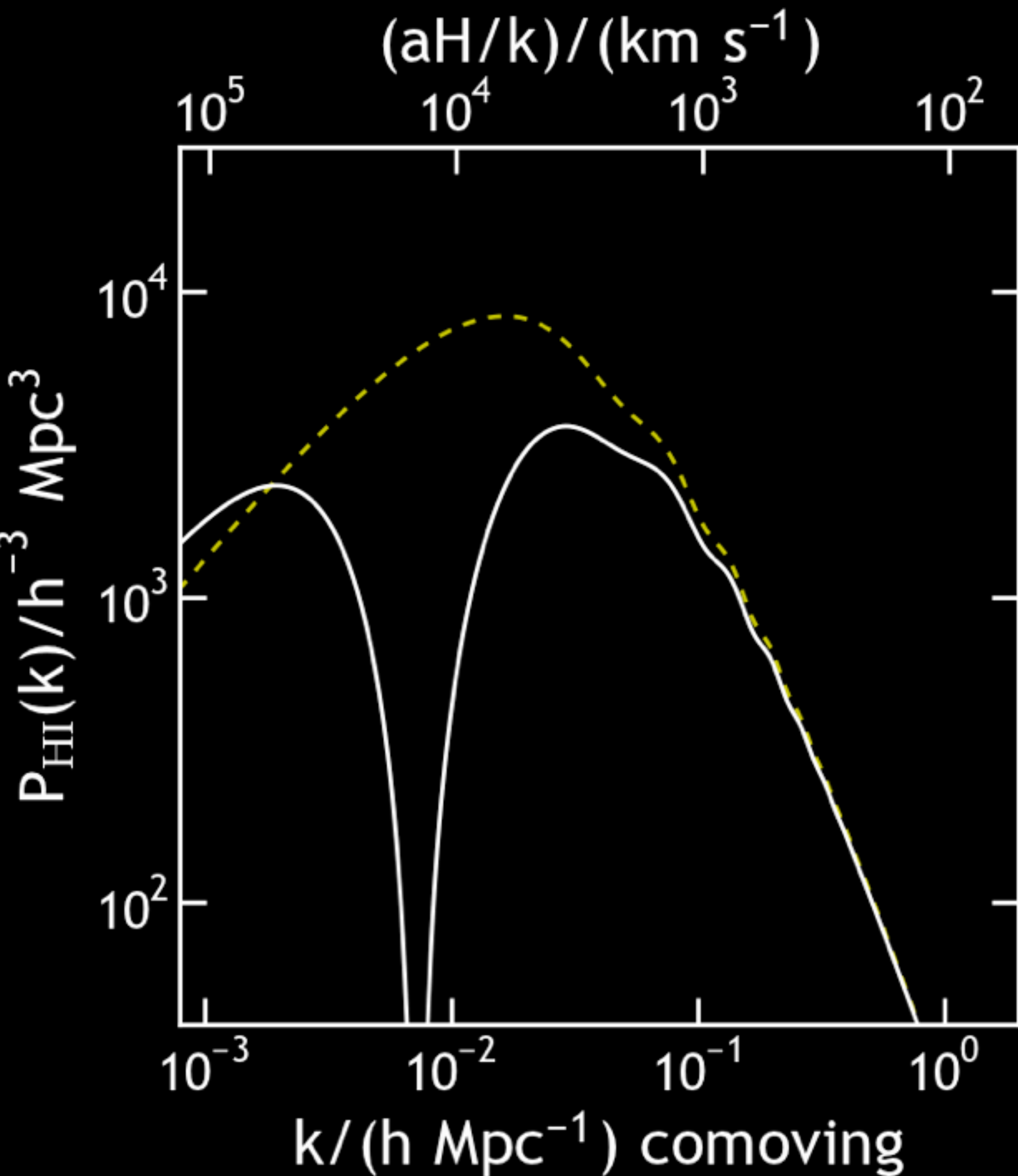

Lyman alpha forest

Uniform UV illumination

Clustered UV illumination (b=3)

Pontzen 2014, PRD
arXiv 1402.0506

see also Gontcho a Gontcho et al 1404.7425

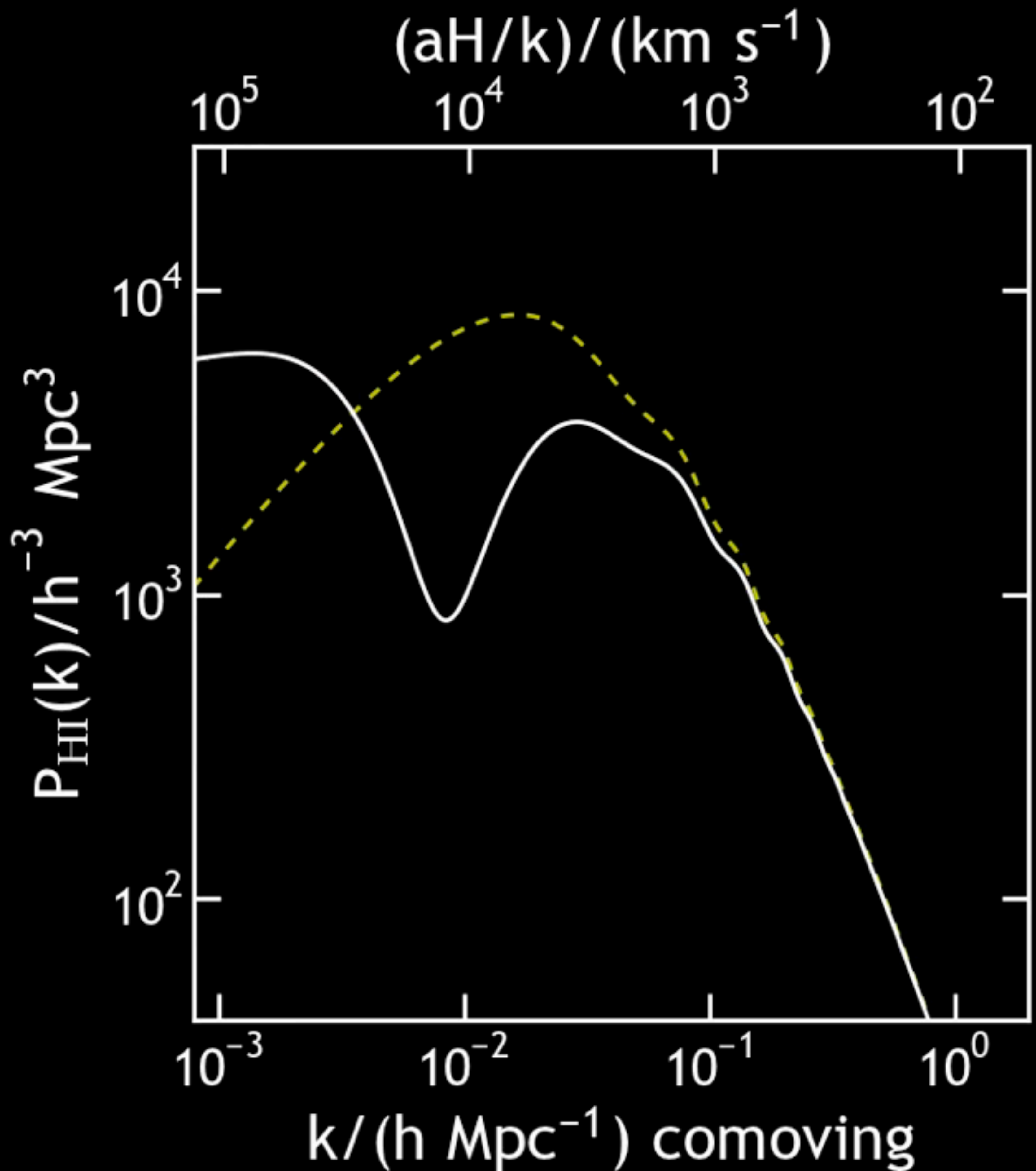

Lyman alpha forest

Uniform UV illumination

Clustered UV illumination (b=3)

+ shotnoise

Pontzen 2014, PRD
arXiv 1402.0506

see also Gontcho a Gontcho et al 1404.7425

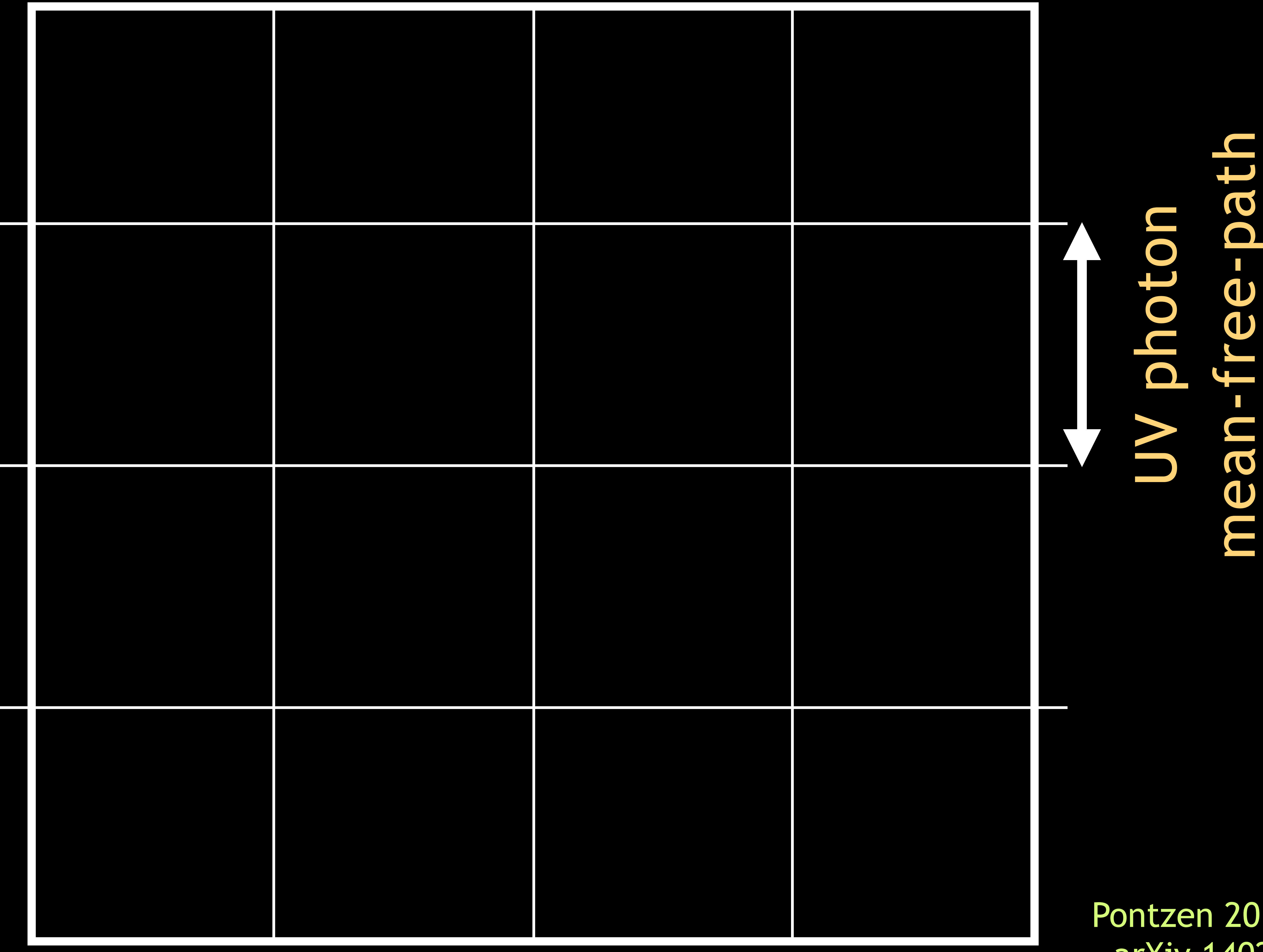

Pontzen 2014, PRD
arXiv 1402.0506

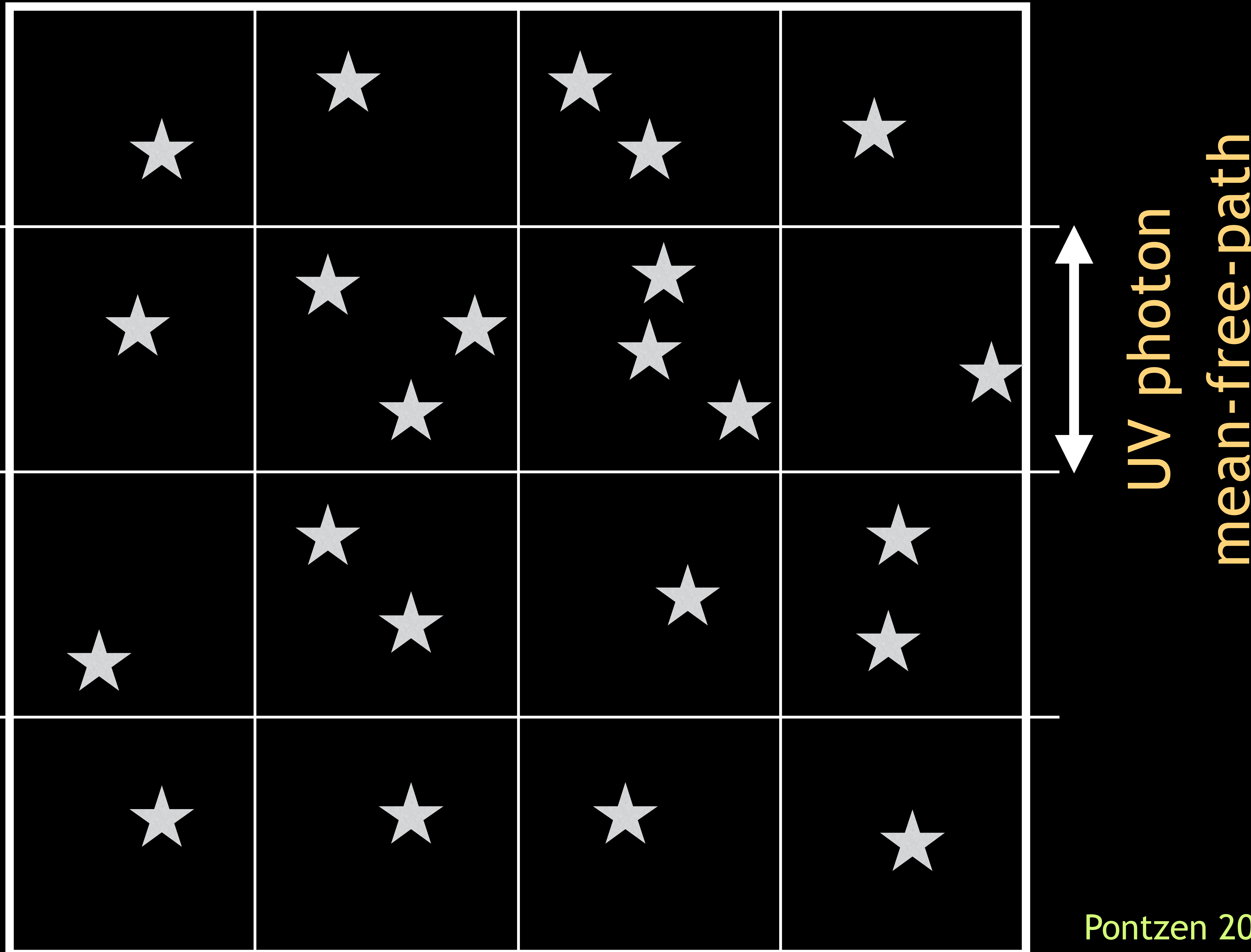

Pontzen 2014, PRD
arXiv 1402.0506

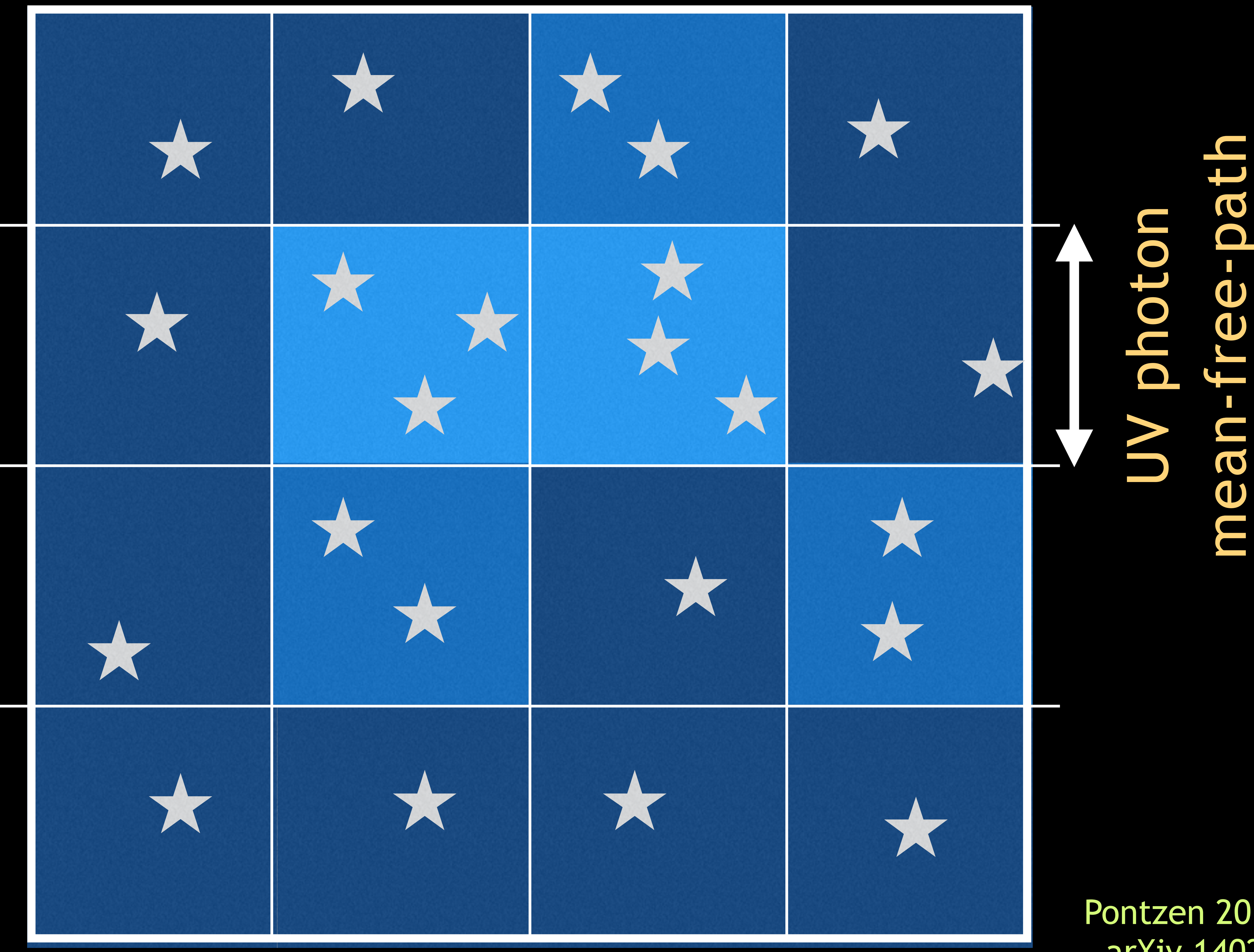

Pontzen 2014, PRD
arXiv 1402.0506

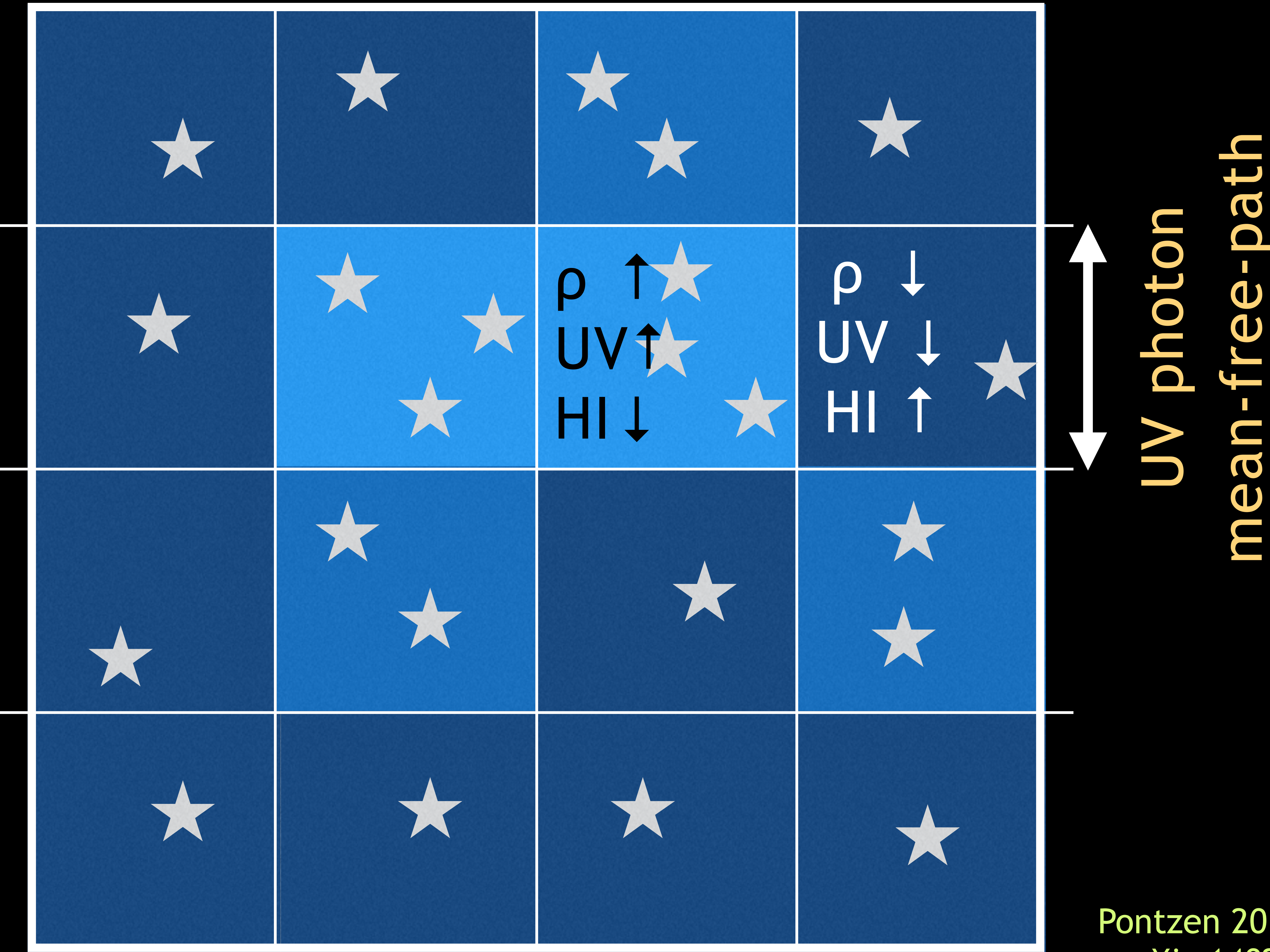

Pontzen 2014, PRD
arXiv 1402.0506

Analytics

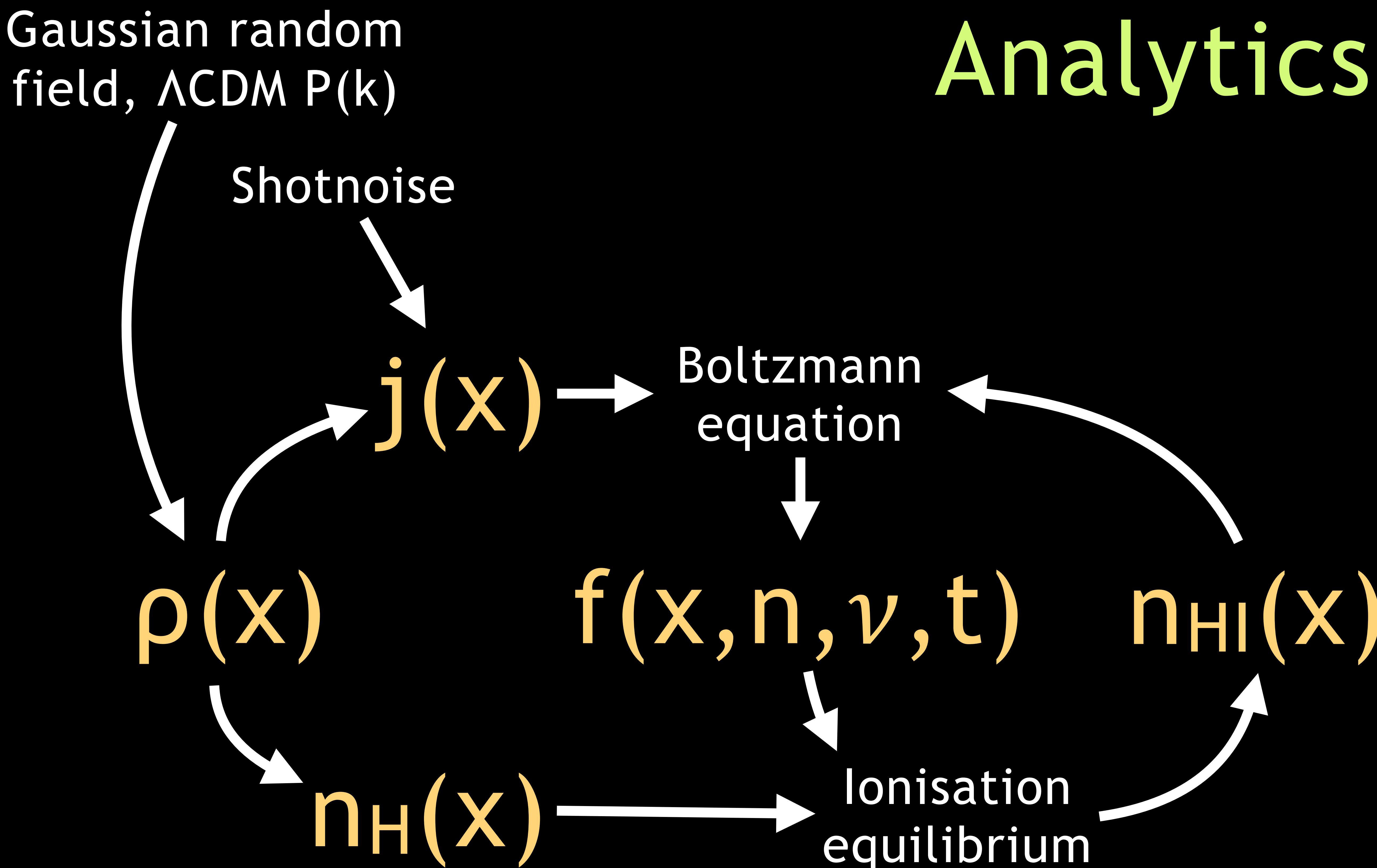

Pontzen 2014, PRD
arXiv 1402.0506

Analytics

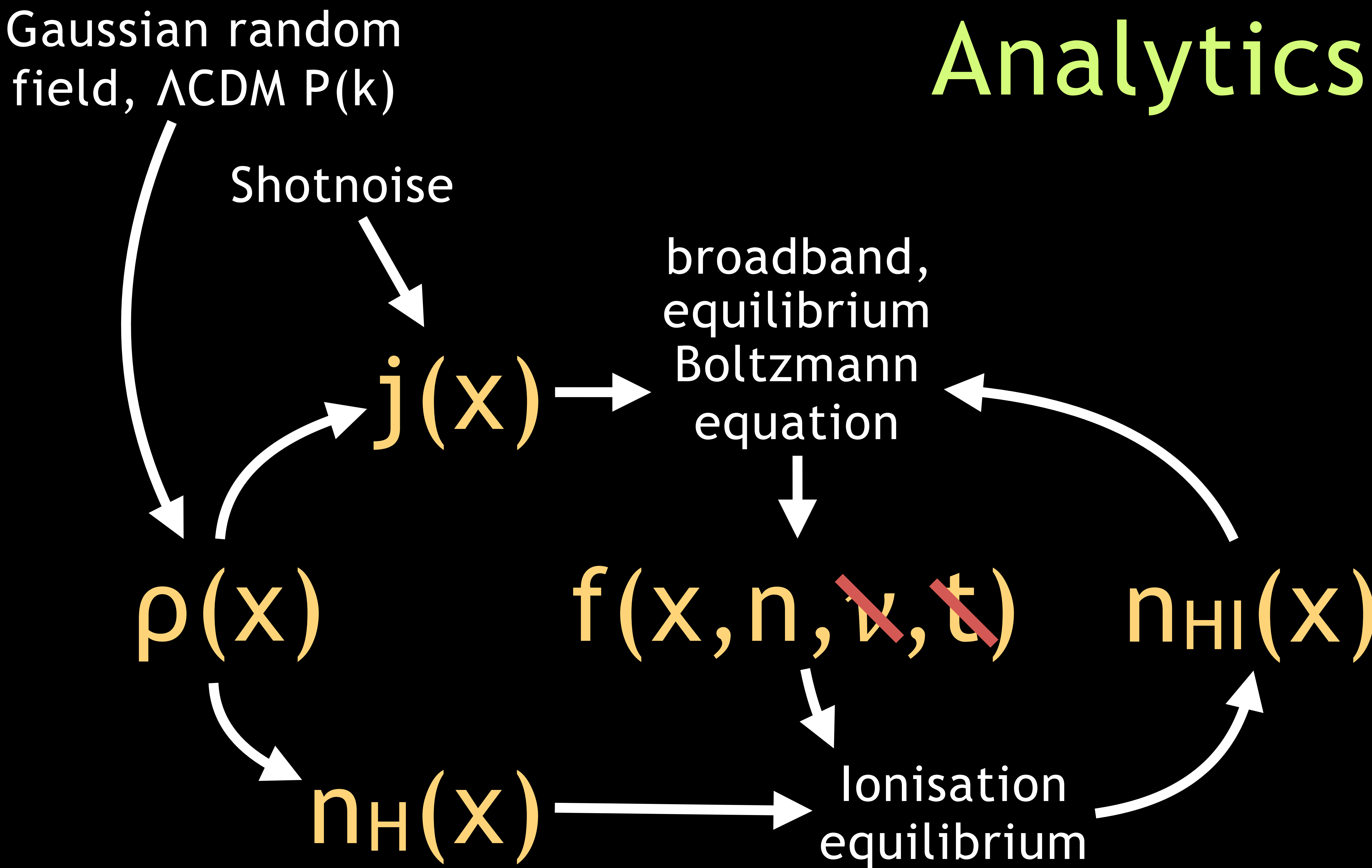

Pontzen 2014, PRD
arXiv 1402.0506

Effect of source bias

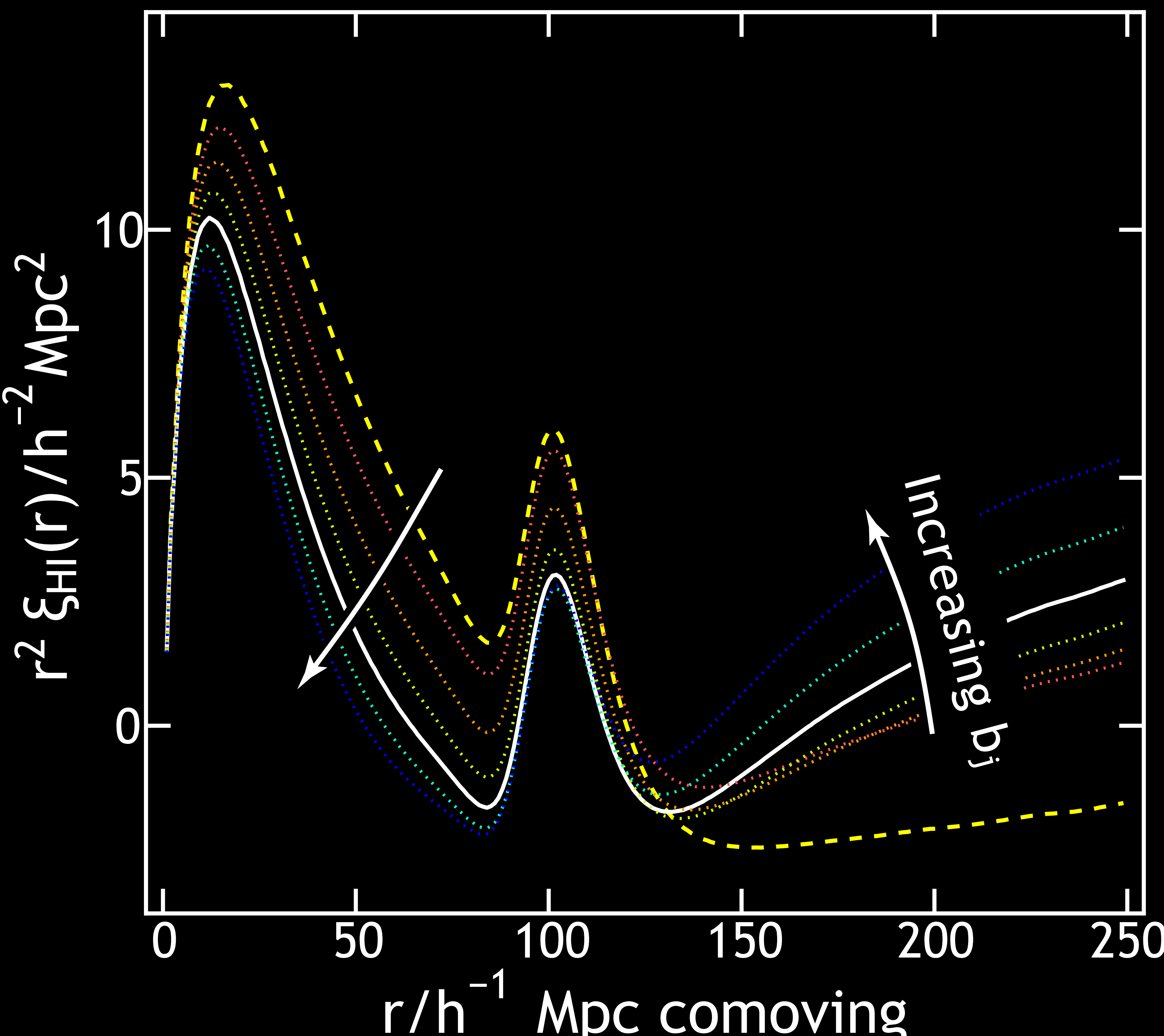

Pontzen 2014, PRD
arXiv 1402.0506

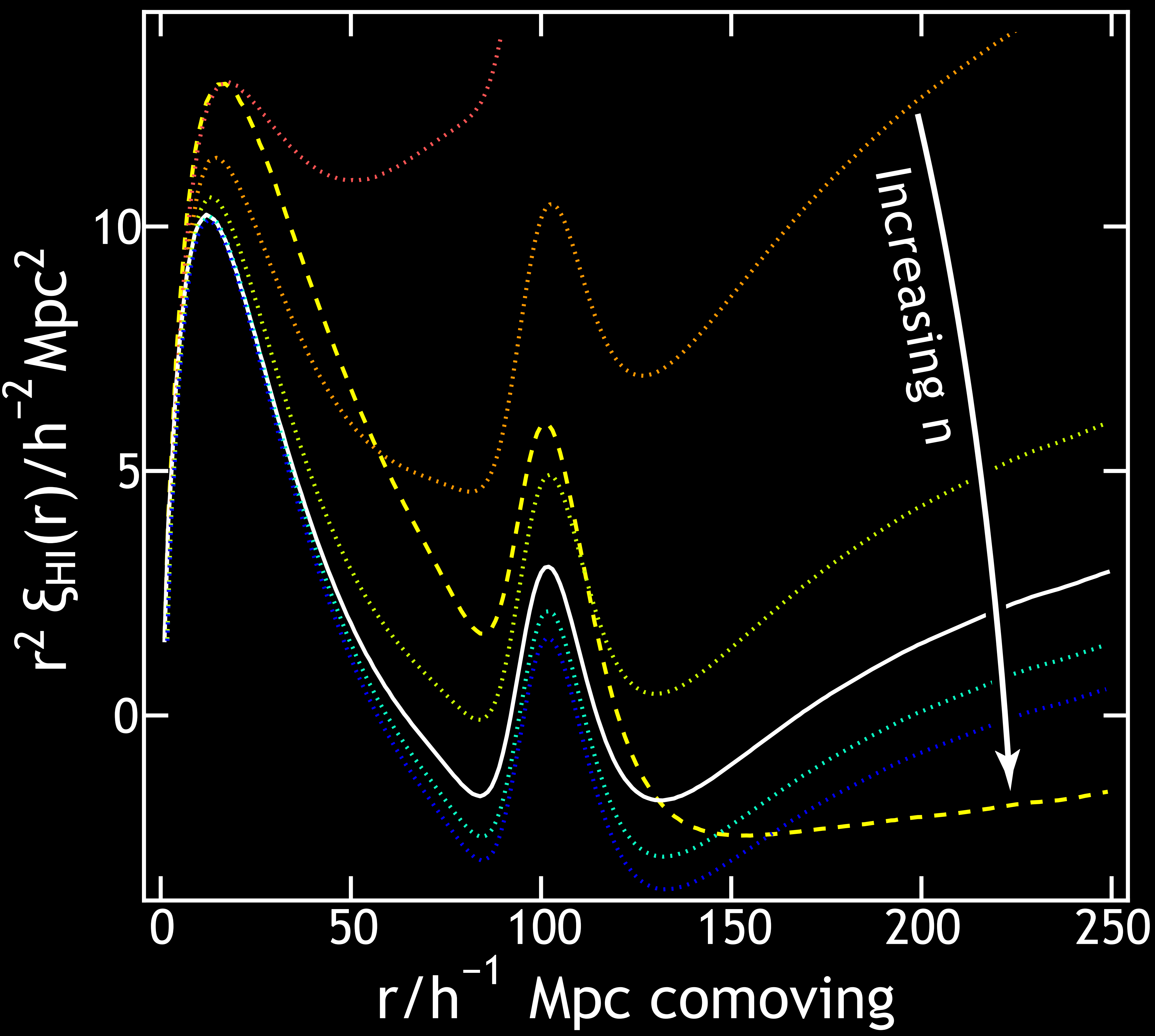

Effect of source density

Pontzen 2014, PRD
arXiv 1402.0506

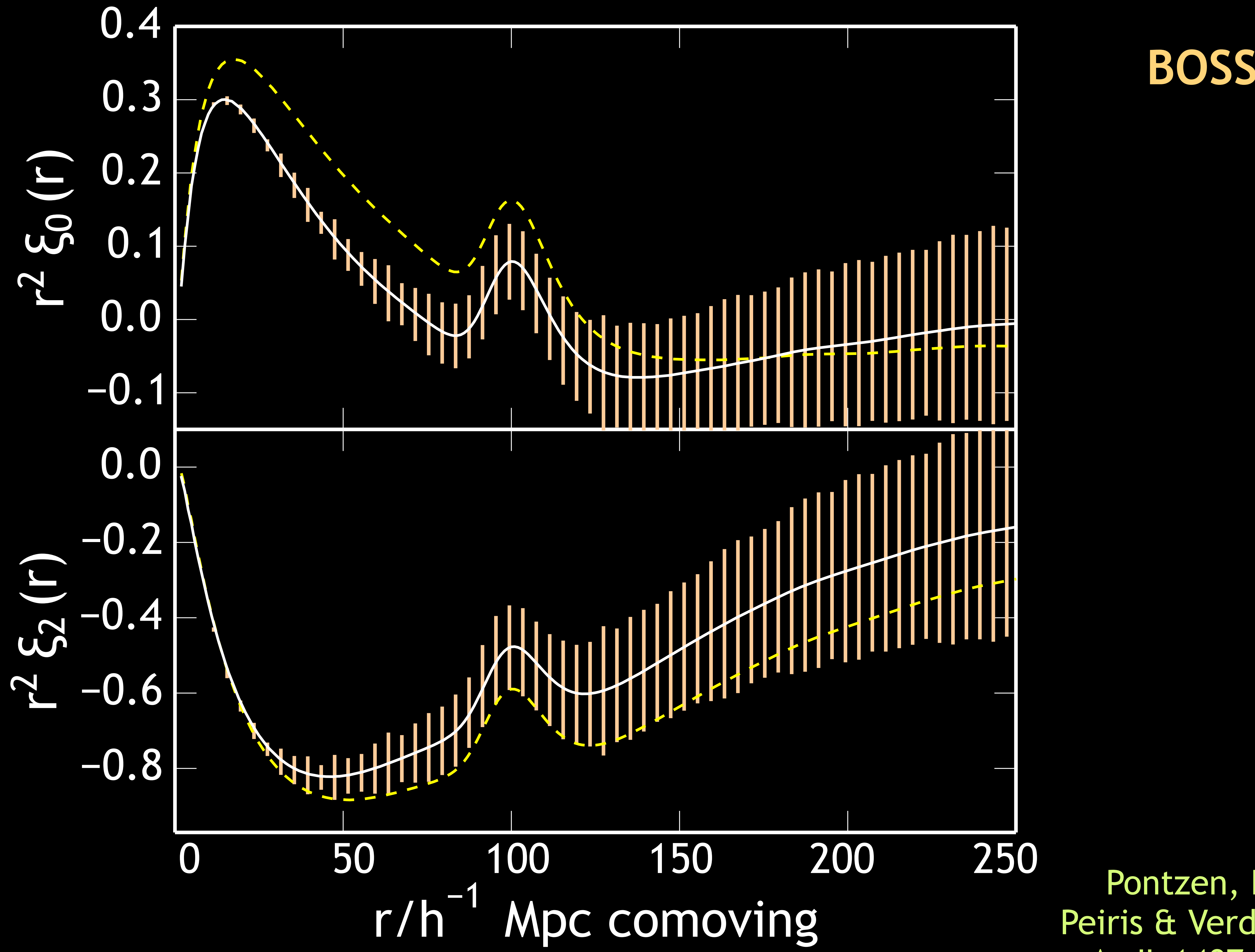

Pontzen, Bird
Peiris & Verde 2014
ApJL 1407.6367

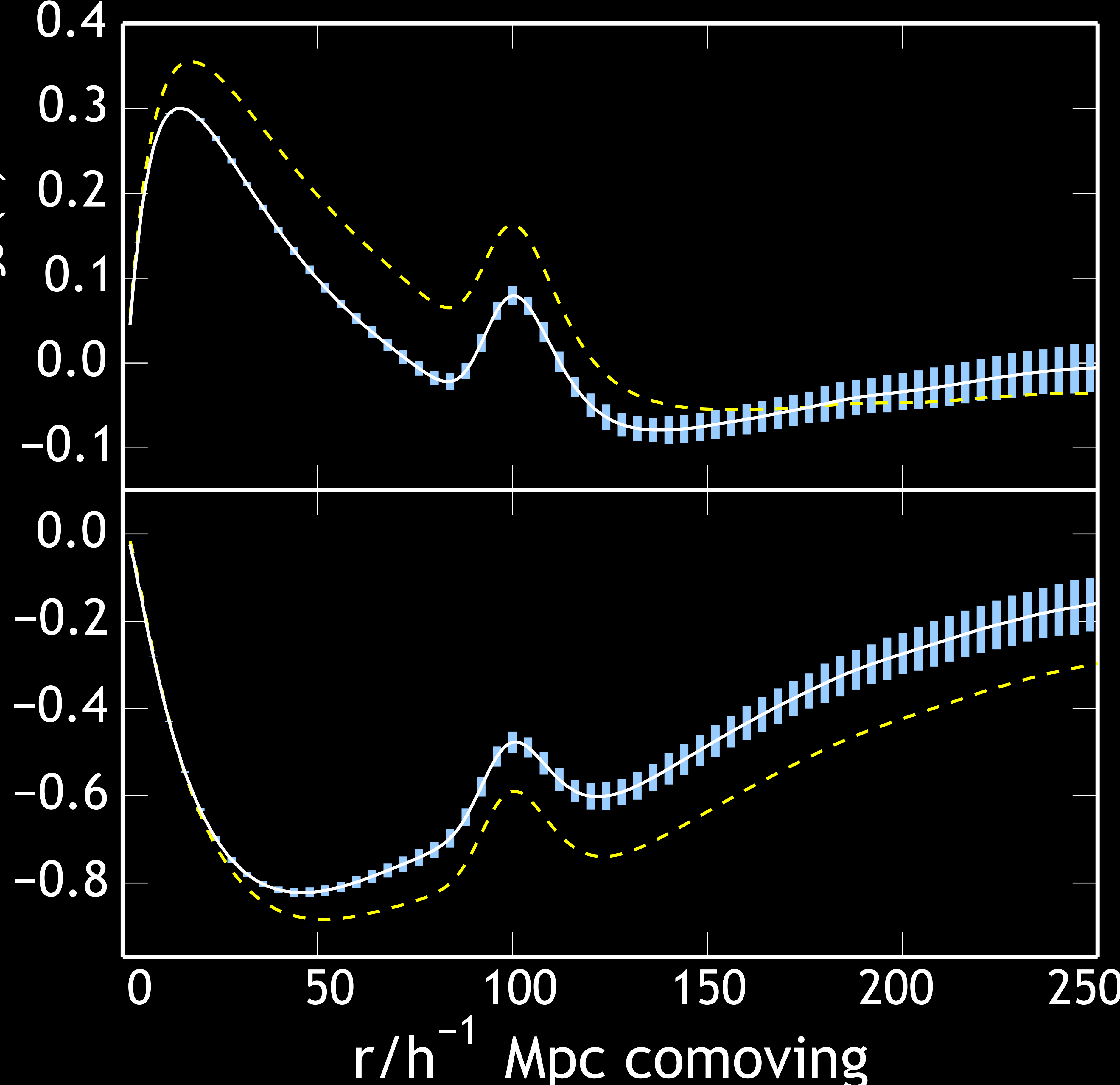

DESI

Pontzen, Bird
Peiris & Verde 2014
ApJL 1407.6367

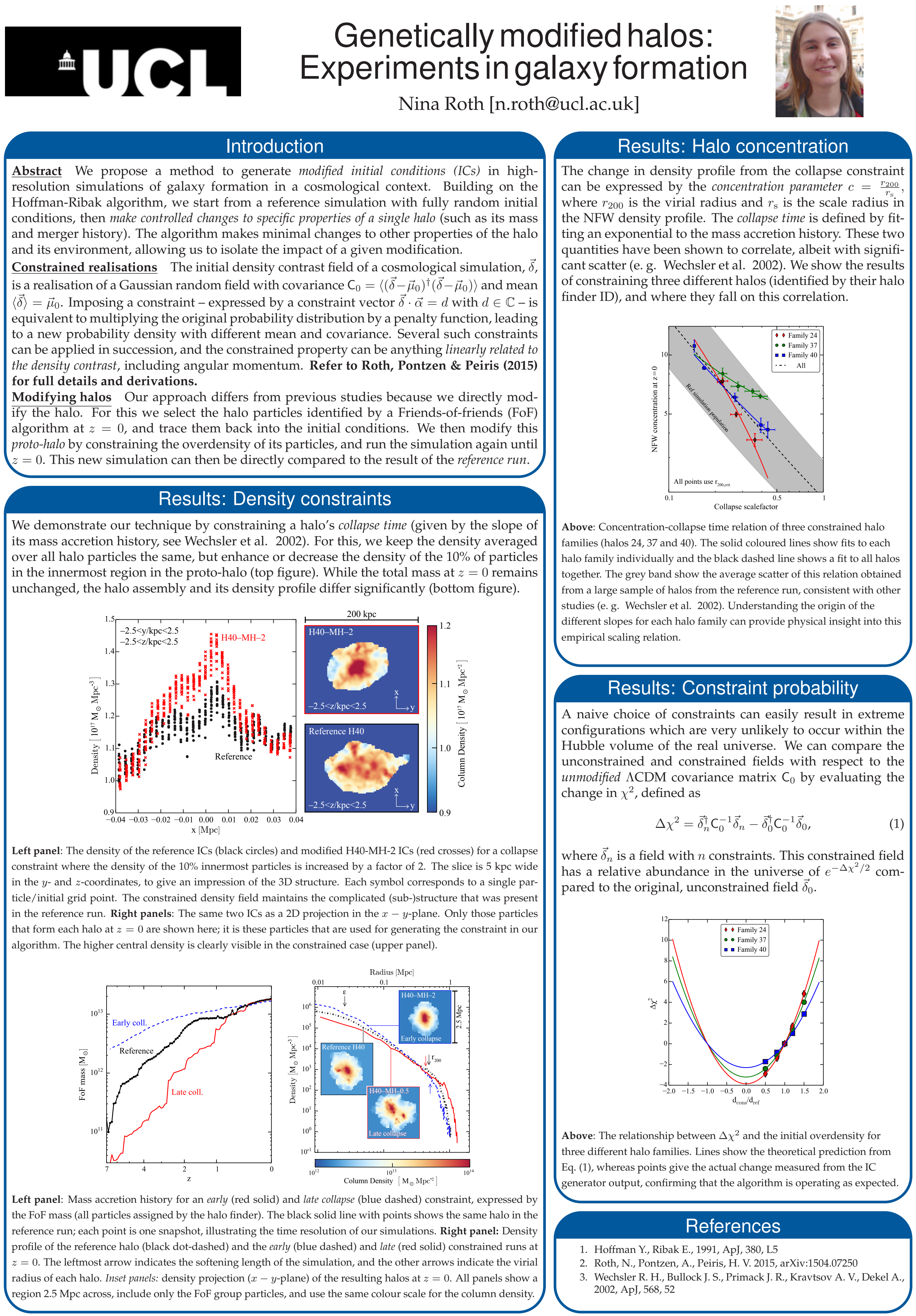

Genetically modified halos: Experiments in galaxy formation

Nina Roth [n.roth@ucl.ac.uk]

Introduction

Abstract We propose a method to generate *modified initial conditions (ICs)* in high-resolution simulations of galaxy formation in a cosmological context. Building on the Hoffman-Ribak algorithm, we start from a reference simulation with fully random initial conditions, then *make controlled changes to specific properties of a single halo* (such as its mass and merger history). The algorithm makes minimal changes to other properties of the halo and its environment, allowing us to isolate the impact of a given modification.

Constrained realisations The initial density contrast field of a cosmological simulation, $\vec{\delta}$, is a realisation of a Gaussian random field with covariance $\mathsf{C}_0 = \langle(\vec{\delta}-\vec{\mu}_0)^\dagger(\vec{\delta}-\vec{\mu}_0)\rangle$ and mean $\langle\vec{\delta}\rangle = \vec{\mu}_0$. Imposing a constraint – expressed by a constraint vector $\vec{\delta}\cdot\vec{\alpha} = d$ with $d \in \mathbb{C}$ – is equivalent to multiplying the original probability distribution by a penalty function, leading to a new probability density with different mean and covariance. Several such constraints can be applied in succession, and the constrained property can be anything *linearly related to the density contrast*, including angular momentum. **Refer to Roth, Pontzen & Peiris (2015) for full details and derivations.**

Modifying halos Our approach differs from previous studies because we directly modify the halo. For this we select the halo particles identified by a Friends-of-friends (FoF) algorithm at $z = 0$, and trace them back into the initial conditions. We then modify this *proto-halo* by constraining the overdensity of its particles, and run the simulation again until $z = 0$. This new simulation can then be directly compared to the result of the *reference run*.

Results: Density constraints

We demonstrate our technique by constraining a halo's *collapse time* (given by the slope of its mass accretion history, see Wechsler et al. 2002). For this, we keep the density averaged over all halo particles the same, but enhance or decrease the density of the 10% of particles in the innermost region in the proto-halo (top figure). While the total mass at $z = 0$ remains unchanged, the halo assembly and its density profile differ significantly (bottom figure).

Left panel: The density of the reference ICs (black circles) and modified H40-MH-2 ICs (red crosses) for a collapse constraint where the density of the 10% innermost particles is increased by a factor of 2. The slice is 5 kpc wide in the y- and z-coordinates, to give an impression of the 3D structure. Each symbol corresponds to a single particle/initial grid point. The constrained density field maintains the complicated (sub-)structure that was present in the reference run. **Right panels**: The same two ICs as a 2D projection in the $x-y$-plane. Only those particles that form each halo at $z = 0$ are shown here; it is these particles that are used for generating the constraint in our algorithm. The higher central density is clearly visible in the constrained case (upper panel).

Left panel: Mass accretion history for an *early* (red solid) and *late collapse* (blue dashed) constraint, expressed by the FoF mass (all particles assigned by the halo finder). The black solid line with points shows the same halo in the reference run; each point is one snapshot, illustrating the time resolution of our simulations. **Right panel:** Density profile of the reference halo (black dot-dashed) and the *early* (blue dashed) and *late* (red solid) constrained runs at $z = 0$. The leftmost arrow indicates the softening length of the simulation, and the other arrows indicate the virial radius of each halo. *Inset panels:* density projection ($x-y$-plane) of the resulting halos at $z = 0$. All panels show a region 2.5 Mpc across, include only the FoF group particles, and use the same colour scale for the column density.

Results: Halo concentration

The change in density profile from the collapse constraint can be expressed by the *concentration parameter* $c = \frac{r_{200}}{r_s}$, where r_{200} is the virial radius and r_s is the scale radius in the NFW density profile. The *collapse time* is defined by fitting an exponential to the mass accretion history. These two quantities have been shown to correlate, albeit with significant scatter (e. g. Wechsler et al. 2002). We show the results of constraining three different halos (identified by their halo finder ID), and where they fall on this correlation.

Above: Concentration-collapse time relation of three constrained halo families (halos 24, 37 and 40). The solid coloured lines show fits to each halo family individually and the black dashed line shows a fit to all halos together. The grey band show the average scatter of this relation obtained from a large sample of halos from the reference run, consistent with other studies (e. g. Wechsler et al. 2002). Understanding the origin of the different slopes for each halo family can provide physical insight into this empirical scaling relation.

Results: Constraint probability

A naive choice of constraints can easily result in extreme configurations which are very unlikely to occur within the Hubble volume of the real universe. We can compare the unconstrained and constrained fields with respect to the *unmodified* ΛCDM covariance matrix C_0 by evaluating the change in χ^2, defined as

$$\Delta\chi^2 = \vec{\delta}_n^\dagger \mathsf{C}_0^{-1}\vec{\delta}_n - \vec{\delta}_0^\dagger \mathsf{C}_0^{-1}\vec{\delta}_0, \tag{1}$$

where $\vec{\delta}_n$ is a field with n constraints. This constrained field has a relative abundance in the universe of $e^{-\Delta\chi^2/2}$ compared to the original, unconstrained field $\vec{\delta}_0$.

Above: The relationship between $\Delta\chi^2$ and the initial overdensity for three different halo families. Lines show the theoretical prediction from Eq. (1), whereas points give the actual change measured from the IC generator output, confirming that the algorithm is operating as expected.

References

1. Hoffman Y., Ribak E., 1991, ApJ, 380, L5
2. Roth, N., Pontzen, A., Peiris, H. V. 2015, arXiv:1504.07250
3. Wechsler R. H., Bullock J. S., Primack J. R., Kravtsov A. V., Dekel A., 2002, ApJ, 568, 52

Poster advert!

Controlled Experiments in Galaxy Formation

Nina Roth

Roth, Pontzen & Peiris (2015)

Ionisation fluctuations dominate the Lyman-alpha forest power spectrum on the **largest** scales. Thermal fluctuations will also be important.

Effects on BAO small and correctable;
but "non-BAO" cosmology needs astrophysical effects to be understood and marginalised

arXiv 1402.0506, 1407.6367

Simeon Bird (CfA), Hiranya Peiris (UCL), Licia Verde (Barcelona)

Andrew Pontzen

THE ROYAL SOCIETY